Clinical Studies

Cancer Research

The FGFR4-G388R Single-Nucleotide Polymorphism Alters Pancreatic Neuroendocrine Tumor Progression and Response to mTOR Inhibition Therapy

Stefano Serra[1], Lei Zheng[2,3], Manal Hassan[5], Alexandria T. Phan[5], Linda J. Woodhouse[4], James C. Yao[5], Shereen Ezzat[2,3], and Sylvia L. Asa[1,3]

Abstract

Pancreatic neuroendocrine tumors (pNET), also known as islet cell tumors, exhibit a wide range of biologic behaviors ranging from long dormancy to rapid progression. Currently, there are few molecular biomarkers that can be used to predict recurrence/metastasis or response to therapy. This study examined the predictive and prognostic value of a single nucleotide polymorphism substituting an arginine (R) for glycine (G) in codon 388 of the FGFR4 transmembrane domain. We established the FGFR4 genotype of 71 patients with pNETs and correlated genotype with biologic behavior. We created an *in vivo* model of pNET with BON1 cells and transfected them with either FGFR4-G388 or FGFR4-R388 to determine the mechanism of action and to examine response to the mTOR inhibitor everolimus. We then validated the predictive results of experimental studies in a group of patients treated with everolimus. FGFR4-R388 is associated with more aggressive clinical behavior in patients with pNETs with a statistically significant higher risk of advanced tumor stage and liver metastasis. Using an orthotopic mouse xenograft model, we show that FGFR4-R388 promotes tumor progression by increasing intraperitoneal spread and metastatic growth within the liver. Unlike FGFR4-G388, FGFR4-R388 BON1 tumors exhibited diminished responsiveness to everolimus. Concordantly, there was a statistically significant reduction in response to everolimus in patients with FGFR4-R388. Our findings highlight the importance of the FGFR4 allele in pNET progression and identify a predictive marker of potential therapeutic importance in this disease. *Cancer Res; 72(22); 5683–91. ©2012 AACR.*

Introduction

Fibroblast growth factor receptors (FGFR) are transmembrane kinases involved in mitogenesis, angiogenesis, and wound healing. Four genes encode a number of receptor isoforms of FGFR-1, -2, -3, and -4 (1). The FGFR family has a highly conserved structure: an extracellular ligand-binding domain, a transmembrane domain, and an intracytoplasmic domain with tyrosine kinase activity (2, 3). Germline FGFR mutations are implicated in developmental defects such as skeletal dysplasias and craniosynostotic syndromes (4). FGFR translocations (5) and somatic mutations (6, 7) have been identified in malignancies and amplification of FGFR4 has been reported in breast and gynecologic cancers (8).

Authors' Affiliations: Departments of [1]Pathology and [2]Medicine, and [3]The Ontario Cancer Institute, Campbell Family Institute for Cancer Research, University Health Network, Toronto, Ontario; [4]The Department of Physical Therapy, Faculty of Rehabilitation Medicine, University of Alberta, Edmonton, Alberta, Canada; and [5]The Department of Gastrointestinal Medical Oncology, The University of Texas MD Anderson Cancer Center, Houston, Texas

Note: Supplementary data for this article are available at Cancer Research Online (http://cancerres.aacrjournals.org/).

Corresponding Author: Sylvia L. Asa, Ontario Cancer Institute, 610 University Ave. #8-319, Toronto, Ontario, Canada M5G-2M9. Phone: 416-340-4802; Fax: 416-340-5517; E-mail: sylvia.asa@uhn.ca

doi: 10.1158/0008-5472.CAN-12-2102

Single-nucleotide polymorphisms (SNP) are the most common genetic variations, representing 90% of sequence differences with an overall frequency of about 1 per 1,000 bases. A polymorphism in FGFR4 (9) characterized by conversion of guanine to adenine at position 1,217 in exon 9 results in the substitution of arginine for glycine at codon 388 in the transmembrane domain; 40% to 50% of Caucasians carry at least one copy of this allele. The FGFR4-R388 allele is associated with poor outcomes in cohorts of sarcoma (10), prostate (11), lung (12, 13), and head and neck carcinomas (14) and in those with advanced and treatment-resistant breast cancer (15). The corresponding mouse SNP accelerates breast cancer progression (16). The mechanisms by which this FGFR4 variant promotes enhanced oncogenesis remain unclear.

FGFR4 interaction with N-cadherin, an adhesion molecule implicated in pancreatic neuroendocrine tumor (pNET) invasion and metastasis, results in downstream activation of PLC-γ, PI3K, and MAPK, thereby promoting cell survival, migration, and invasion (17, 18). In this report, we examine the impact of the FGFR4-G388R SNP on pNET progression and response to therapy.

Materials and Methods

Human pNETs

Human pNETs and normal tissue were obtained following informed consent and approval by Institutional Review Committees. Only pNETs classified as G1 and G2 using the 2010

WHO classification (19) were included; poorly differentiated neuroendocrine carcinomas, G3, were excluded. Patients enrolled in a clinical trial of everolimus (20) were examined for correlations between genotype and response.

Genotyping

DNA was isolated from normal somatic tissue or blood using proteinase K digestion and phenol–chloroform extraction. FGFR4 polymorphisms were amplified by PCR as described (9) and sequenced.

Cell lines and cultures

Human pancreatic BON1 cells propagated in Dulbecco's Modified Eagle's Medium (DMEM, Life Technologies, Inc.) with high glucose, 10% FBS, 2 mmol/L glutamine, 100 IU/mL penicillin, and 100 μg/mL streptomycin were serum-starved overnight and treated with FGF-1 (25 ng/mL) or insulin (300 nmol/L) for 15 minutes. The cells were treated with everolimus (10–40 nmol/L; LC laboratories).

Plasmid construction and transfection

Plasmids containing coding regions of human FGFR4-G388 or FGFR4-R388 were stably transfected into the pcDNA3.1 expression vector (Invitrogen; ref. 18). Three clones of cells expressing each isoform or transfected with empty vector were selected for analyses.

Western blotting

Equal amounts of protein separated by 8% SDS-PAGE were transferred onto polyvinylidene difluoride (PVDF) membranes (Millipore). Blots were incubated with polyclonal antiserum against FGFR4 (Santa Cruz) or monoclonal antibody to the V5-tag (Invitrogen), N-cadherin (BD Tranduction Laboratories), STAT3, p-STAT3, AKT, and pS473-AKT (Cell Signaling). Actin (1:500, Sigma) was a loading control. Nonspecific binding was blocked with 5% nonfat milk in 1× Tris-buffered saline (TBST with 0.1% Tween-20). After washing 3 × 10 minutes in 1× TBST, blots were exposed to secondary antibody (antimouse or rabbit IgG-HRP, Santa Cruz Biotechnology) at 1:2,000 and visualized using ECL chemiluminescence (Amersham).

In vivo tumor growth assay

Female severe combined immunodeficient mice (SCID) mice 6 to 7 weeks old were maintained under pathogen-free conditions. For each experiment, 15 mice representing 3 groups (FGFR4-G388, FGFR4-R388, or controls) were injected with 5×10^6 cells. In the subcutaneous model, tumors were measured using vernier calipers (Fisher Scientific Ltd.). In the orthotopic model, imaging with Micro-CT was conducted to assess tumor growth. For mTOR inhibition, everolimus was administered 5 mg/kg intraperitoneally twice weekly.

Following institutional guidelines for ethical care of animals, experiments ended when tumor volumes exceeded 100 mm^3, typically 30 days after implantation. Tumor volumes were calculated as (length × width × depth)/2. Tumors were weighed at autopsy; in the orthotopic model, intraperitoneal dissemination, diaphragmatic and organ involvement, and hemoperitoneun were recorded. Tumor tissue, liver, and lungs were fixed in formalin, and portions of tumors were snap-frozen in liquid nitrogen and stored at −70°C.

Morphology and immunohistochemistry

Sections of formalin-fixed paraffin-embedded tissue were stained with hematoxylin and eosin, or used for immunohistochemical localization with the avidin–biotin complex technique. Immunostaining was conducted in paraffin sections incubated with primary antibodies to various hormones, N-cadherin (BD Tranduction Laboratories, Clone 32, 610921) and Ki67 (MIB-1 polyclonal, Novus Biological NB110-90592). Apoptosis was detected in paraffin sections using the terminal dUTP nick-end labeling (TUNEL) technique.

Statistical analysis

Baseline demographics and characteristics of the study participants were examined using univariate analyses. Data are presented as mean ± SD. In experimental models, differences were assessed using independent, 2-sided *t* tests. Analysis of surgical human tumor specimens applied Fisher exact test. Correlational analyses were used to examine relationships among variables. Multiple logistic regression was then used to identify which variables were associated with the development of liver metastases. Analyses were conducted using SPSS version 19 (SPSS Inc.). All differences were deemed to be significant at $P \leq 0.05$. Progression-free survival (PFS) and overall survival (OS) were estimated by the Kaplan–Meier method, and the log-rank test was used to compare the difference between patient or genotype groups. The hazard ratio (HR) between 2 groups was estimated by proportional hazards regression with a 95% Wald confidence interval (95% CI). Data analysis was done with SAS version 9.2, and all *P* values were 2 sided.

Results

Primary human pNETs

Clinicopathologic features. The 71 patients (Supplementary Table S1), 31 men (43.7%) and 40 women, ranged from 23 to 80 (mean 52.3) years of age. Tumors measured 0.8 to 11.0 cm; 20 were 2 cm or less. Eight patients had multiple tumors and familial cancer syndromes; 7 had multiple endocrine neoplasia type I (MEN-I) and 1 had von Hippel–Lindau disease. Ten patients had clinical evidence of hormone hypersecretion; all were insulinomas (Supplementary Table S1).

Immunohistochemistry identified insulin in 25 tumors; only 10 were clinical insulinomas. Glucagon was found in 13, 9 expressed gastrin, 8 serotonin, and 7 vasoactive intestinal peptide (VIP). Twenty-two expressed 2 or more hormones and 14 were negative for hormones. The mitotic rate was 0 to 12/10 high power fields (HPF). Twelve had greater than 2 mitoses/10 HPF. The Ki-67 labeling index ranged from less than 1% to 20%; 18 were greater than 2%. Twenty-one tumors exhibited local invasion into peripancreatic fat; 32 displayed angioinvasion. Seventeen had lymph node metastases, and 12 had liver metastases.

Genetic analysis. Genotyping showed that 35 (49.3%) patients were homozygous for FGFR4-G388, 30 (42.3%) were heterozygous, and 6 (8.5%) were homozygous for FGFR4-R388.

Genotype and hormone expression. Although there was no statistically significant correlation between genotype and hormone production (Table 1), among clinical insulinomas, 7 (70%) were homozygous FGFR4-G388, whereas only 3 (30%) had an FGFR4-R388 allele. Among 13 tumors that expressed glucagon, 9 (69%) were FGFR4-G388 homozygous, whereas 4 (31%) carried an FGFR4-R388 allele. Nine tumors expressed gastrin; 5 (56%) were FGFR4-G388 homozygous and 4 (44%) had an FGFR4-R388 allele. Eight tumors expressed serotonin; 5 (63%) were homozygous FGFR4-G388 and 3 (37%) had an FGFR4-R388 allele. Seven tumors were positive for VIP; only 2 (29%) were homozygous FGFR4-G388, whereas 5 (71%) had an FGFR4-R388 allele.

Genotype and N-cadherin expression. To determine if FGFR4 genotype altered N-cadherin expression in these tumors, we conducted immunohistochemistry for N-Cadherin in 69 cases where remaining tissue was available. Of the 40 positive cases, 23 (58%) carried an FGFR4-R388 allele, whereas 42% were homozygous FGFR4-G388. N-Cadherin expression was cytoplasmic in the majority of cases studied. Only 4 cases, 3 homozygous FGFR4-G388, and 1 homozygous FGFR4-R388 showed a membranous staining pattern. There was no significant correlation between FGFR4 genotype and N-Cadherin expression.

Genotype and tumor aggressiveness. Tumor size was unknown in 6 cases. Of 20 tumors less than 2 cm, 11 (55%) were homozygous FGFR4-G388, 6 (30.0%) were heterozygous, and 3 (15.0%) were homozygous FGFR4-R388. In contrast, of 45 tumors $\geq$2 cm, 21 (47%) were heterozygous, whereas 3 (6%) were homozygous for FGFR4-R388 and 21 (47%) were homozygous FGFR4-G388. Interestingly, 55.0% of patients with pNETS less than 2 cm were homozygous FGFR4-G388, whereas 53% of patients with pNETs $\geq$2 cm had an FGFR4-R388 allele (Table 1).

Mitotic count was unknown in one case. Of 20 pNETs with 2 to 20/10 HPF, 9 (45%) were homozygous FGFR4-G388, 10 (50%)

Table 1. Tumor parameters and FGFR4 genotype

Parameter	Variable	Number	G/G (%)	G/R or R/R (%)
Hormone status	Insulinoma[a]	10	7 (70)	3 (30)
	Noninsulinoma[a]	61	28 (46)	33 (54)
	Insulin +	25	12 (48)	13 (52)
	Insulin −	46	23 (50)	23 (50)
	Glucagon +	13	9 (69)	4 (31)
	Glucagon−	58	26 (45)	32 (55)
	Gastrin +	9	5 (56)	4 (44)
	Gastrin −	62	30 (48)	32 (52)
	Serotonin +	8	5 (63)	3 (37)
	Serotonin −	63	30 (48)	33 (52)
	VIP +	7	2 (29)	5 (71)
	VIP −	64	33 (52)	31 (48)
Tumor size	<2 cm	20	11 (55)	9 (45)
	$\geq$2 cm	45	21 (47)	24 (53)
Mitoses	<2/HPF	50	26 (52)	24 (48)
	2–20/HPF	20	9 (45)	11 (55)
MIB-1 labeling index	$\leq$2%	44	22 (50)	22 (50)
	3%–20%	18	8 (44)	10 (56)
Grade	G1	43	23 (54)	20 (46)
	G2	27	12 (44)	15 (56)
Local invasion	Confined to pancreas	49	25 (51)	24 (49)
	Locally invasive	21	10 (48)	11 (52)
Lymphovascular invasion	Not identified	38	20 (53)	18 (47)
	Present	32	15 (47)	17 (53)
Lymph node status	Negative	53	29 (55)	24 (45)
	Positive	17	6 (35)	11 (65)
Liver metastases[b]	Negative	59	33 (56)	26 (44)
	Positive	12	2 (17)	10 (83)
Stage	I	36	19 (53)	17 (47)
	II	21	13 (62)	8 (38)
	IV	12	2 (17)	10 (83)

[a]Defined by clinical function, not immunoprofile; + positive; − negative.
[b]Statistically significant difference by genotype in univariate analysis, $P = 0.013$.

were heterozygous, and 1 (5%) was homozygous FGFR4-R388. Of 50 patients whose pNETs had less than 2 mitoses/10 HPF, 26 (52%) were homozygous FGFR4-G388, 19 were heterozygous, and 5 were homozygous FGFR4-R388; 24 (48%) had an R388 allele.

The MIB-1 labeling index was unknown in 9 cases. Among patients with tumor MIB-1 2% to 20%, 8 (44%) were homozygous FGFR4-G388, 8 were heterozygous, and 2 were homozygous FGFR4-R388; 56% harbored an R388 allele. Of 44 patients with tumor MIB-1 less than equal to 2%, 22 (50%) were homozygous FGFR4-G388, 18 (41%) were heterozygous, and 4 (9%) were homozygous FGFR4-R388.

Tumor grade. Tumors were divided according to the 2010 WHO into Grade 1 (G1) and Grade 2 (G2); no poorly differentiated Grade 3 (G3) tumors were included in this study. The grade of 1 tumor was not known. Among patients with G2 tumors, 12 (44%) were homozygous FGFR4-G388, 13 (48%) were heterozygous, and 2 were homozygous FGFR4-R388; 56% harbored an R388 allele. Of the 43 patients with G1 tumors, 23 (54%) were homozygous FGFR4-G388, 16 (37%) were heterozygous, and 4 (9%) were homozygous FGFR4-R388.

The status of local invasion was unclear in one case. Forty-nine patients had tumors confined to pancreas; 25 (51%) were homozygous FGFR4-G388, 21 (43%) heterozygous, and 3 (6%) homozygous FGFR4-R388. Of 21 patients with locally invasive pNETs, 10 (48%) were homozygous FGFR4-G388, 8 (38%) were heterozygous, and 3 (14%) were homozygous FGFR4-R388.

Lymphovascular invasion was unknown in one case. Of 32 patients with lymphovascular invasion, 15 (47%) were FGFR4-G388 homozygotes, 14 (48%) heterozygotes, and 3 (9%) were FGFR4-R388 homozygotes. In contrast, of 38 patients with nonangioinvasive pNETs, 20 (53%) were FGFR4-G388 homozygotes, 15 (39%) heterozygotes, and 3 (8%) were FGFR4-R388 homozygotes. Therefore, 53% of angioinvasive pNETs were in FGFR4-R388 carriers, whereas 53% of nonangioinvasive pNETs were from FGFR4-G388 homozygotes.

Of 17 patients with lymph node involvement, only 6 (35%) were homozygous FGFR4-G388, whereas 9 (53%) were heterozygous and 2 (12%) were homozygous FGFR4-R388. In contrast, of 53 patients without lymph node involvement, 29 (55%) were homozygous FGFR4-G388, 20 (38%) heterozygous, and 4 (7%) were homozygous FGFR4-R388. Although not statistically significant due to small numbers, it is notable that the FGFR4-R388 allele, which is usually present in less than 50% of the population, was present in 11 of 17 (65%) patients who developed lymph node metastasis.

Of 12 pNETs with liver metastasis, 8 were heterozygous FGFR4-R388 and 2 were homozygous; only 2 were homozygous FGFR4-G388. Of 59 patients that had no liver metastasis, 33 were homozygous FGFR4-G388, 5 were homozygous FGFR4-R388; the remainder were heterozygous. Most importantly, the FGFR4-R388 allele was present in 83% of the pNETs with liver metastasis. This was statistically significant ($P = 0.013$).

Tumor stage was unknown in 2 cases. Of the patients with stage I and II disease, 19 (53%) and 13 (62%) were homozygous FGFR4-G388, respectively, and 17 (47%) and 8 (38%) had an FGFR4-R388 allele. No patient had stage III disease. Of the 12 patients with stage IV disease, 2 were homozygous FGFR4-R388, 8 were heterozygous, and 2 were homozygous FGFR4-G388. Therefore, the FGFR4-R388 allele was present in 83% (10/12) of the stage IV pNETs, reaching statistical significance ($P = 0.036$).

Risk of liver metastases. In our series, the probability of developing liver metastases was 16.9% (12/71). The percentage of patients who developed liver metastases with an FGFR4-R388 allele was 27.8% (10/36) compared with 5.7% (2/35) for FGFR4-G388 homozygotes (Table 2). The estimated risk of developing liver metastases in FGFR4-R388 carriers compared with FGFR4-G388 was 6.3 (95%CI: 1.3–31.5; Table 2). Regression analysis confirmed the value of FGFR4-R388 as a predictive marker for liver metastases. Multiple logistic regression revealed a statistically significant ($P < 0.0001$) 3-variable model including lymphovascular invasion (OR 13.8, 95%CI: 1.5–128.0), presence of lymph nodes metastases (OR 5.0, 95%CI: 1.0–24.8), and FGFR4 genotype (homozygous or heterozygous FGFR4-R388 vs. FGFR4-G388 OR 5.7, 95%CI: 0.9–34.7) that was associated with the development of liver metastasis.

In vivo tumor growth assay

To examine the biologic impact of the FGFR4 SNP, we introduced either FGFR4-G388 or FGFR4-R388 into pancreatic NET BON1 cells that have endogenous FGFR4-G388.

Table 2. FGFR4 genotype and risk of liver metastasis

	Liver metastases		
Risk factor	**Negative $n = 59$ (%)**	**Positive $n = 12$ (%)**	**OR (95% CI)**
Lymphovascular invasion			
No	37 (62.7)	1 (0.09)	1 (reference)
Yes	22 (37.3)	10 (90.9)	16.8 (2.0–140.4)
Lymph node metastases			
No	49 (83.1)	4 (36.4)	1 (reference)
Yes	10 (16.9)	7 (63.6)	8.6 (2.1–34.9)
FGFR4 genotype			
FGFR4-G388 (G/G)	33 (55.9)	2 (16.7)	1 (reference)
FGFR4-R388 (G/R or R/R)	26 (44.1)	10 (83.3)	6.3 (1.3–31.5)

In the subcutaneous flank model, the median tumor burden was significantly higher in FGFR4-R388 than in FGFR4-G388 tumors (952 vs. 688 mm^3; $P = 0.05$) or control tumors (median 603 mm^3; $P = 0.05$; Fig. 1A). Tumor weights were significantly greater in FGFR4-R388 compared with FGFR4-G388 tumors (Fig. 1B).

The orthotopic model recapitulated the human disease with tumor nodules in pancreas and peripancreatic tissue and spread into mesentery (Fig. 1C and D). Bloody ascites developed exclusively in 5/16 (31.2%) FGFR4-R388 tumors ($P = 0.001$). Tumor deposits on the abdominal surface of the diaphragm developed in 6/16 (37.5%) FGFR4-R388 tumors, 2/18 (11%) control tumors, and in no FGFR4-G388 tumors ($P = 0.006$). Lung metastases developed in 3/16 (18.7%) FGFR4-R388 tumors and 2/18 (11%) controls, but not in FGFR4-G388 tumors, yielding a statistically significant difference between FGFR4-R388 and FGFR4-G388 tumors ($P = 0.034$). Liver metastases were significantly more frequent with FGFR4-R388 tumors (5/16, 31.2%) compared with FGFR4-G388 (1/20, 5%; $P = 0.019$). Liver metastases developed in 2/18 (11%) controls.

The median weight of intraperitoneal metastases was significantly higher in FGFR4-R388 tumors compared with FGFR4-G388 and control tumors (1.37, 0.81, and 0.70 g, respectively; $P = 0.017$; Fig. 1E). Primary tumor weights were also heavier in FGFR4-R388 compared with FGFR4-G388 tumors (0.67 vs. 0.43g; $P = 0.05$) but were not statistically greater than controls (0.59 g).

In all experiments, histology confirmed the presence of tumor nodules composed of large cells with abundant eosinophilic cytoplasm and large nuclei with "salt and pepper" chromatin, arranged in nests and sheets. The neoplastic cells were positive for chromogranin, validating the model of neuroendocrine carcinoma. There was no morphologic difference between tumors of different genotypes. The Ki67 labeling index was 60% to 70% and there were 32 to 58 mitoses per 10 HPF, however, it is difficult to compare these parameters in a cell line model with the primary human tumor situation. There was no significant difference in Ki67 labeling index, apoptosis as detected by TUNEL, or N-cadherin expression by Western blotting or immunohistochemistry associated with genotype.

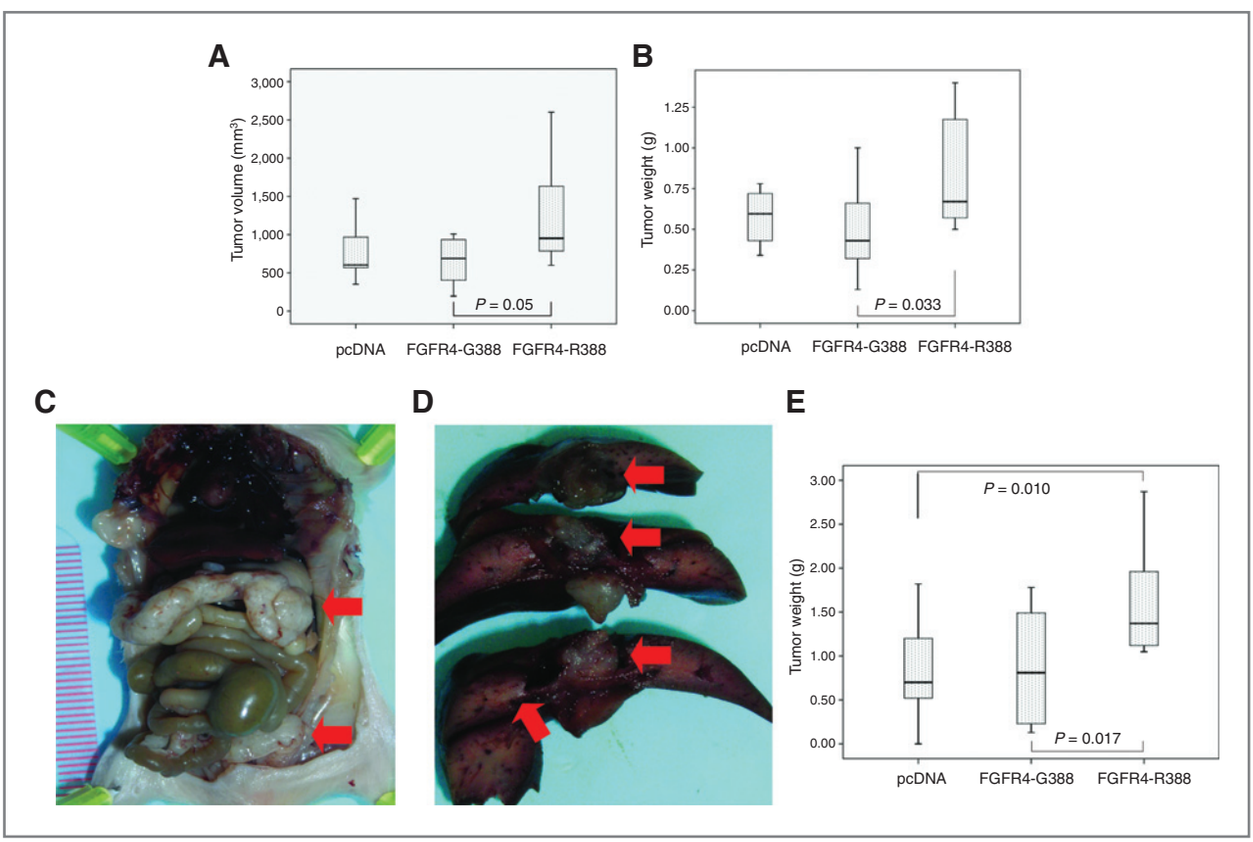

Figure 1. The FGFR4 SNP alters pNET progression in mouse xenografts. A and B, human pancreatic neuroendocrine BON1 cells stably expressing the FGFR4-G388, the polymorphic form of the receptor FGFR4-R388, or their empty vector (pcDNA) control were examined in flank xenografted SCID mice as detailed in Materials and Methods. Data represent the mean of 2 independent experiments, each including 5 mice per group. A, statistically significant differences ($P = 0.05$) in tumor volumes are identified. B, corresponding changes in tumor weights measured at the time of sacrificing show a statistically significant increase in the FGFR4-R388 group. C–E, pancreatic neuroendocrine BON1 cells as described in A and B were introduced orthotopically into the peritoneal cavity of SCID mice. This orthotopic model results in pancreatic tumors (top arrow; C) with peritoneal spread (bottom arrow; C) and liver metastases (arrows; D). The tumor weights (E) expressed as means of measurements obtained from 2 independent experiments, each with 5 mice in each group identify statistically significant differences in tumor weight ($P < 0.05$) based on FGFR4 genotype.

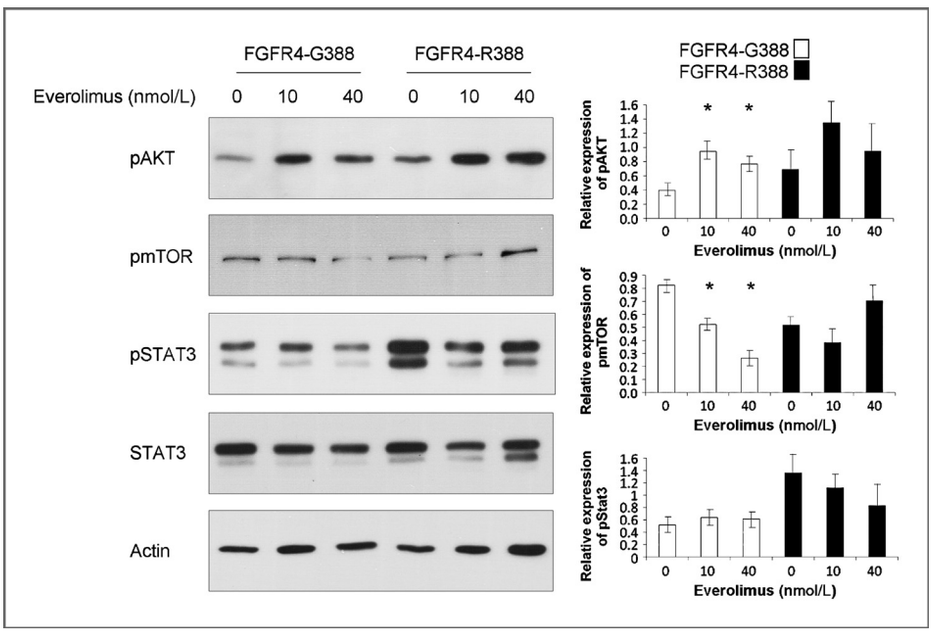

Figure 2. Comparison of signaling potential of BON1 cells expressing different FGFR4 isoforms. BON1 cells expressing FGFR4-G388 or FGFR4-R388 were treated with the indicated doses of the mTOR inhibitor everolimus for 24 hours as detailed in Materials and Methods. Total cell lysates were resolved on 8% SDS gels and transferred to membranes for hybridization with the indicated antibodies. Signal intensities were quantified by densitometric measurements. Values depicted in the bar graphs at right represent the mean of triplicate experiments of phosphorylated proteins adjusted for total protein of the indicated type; *, statistical significance of differences between control and treated cells. Unlike FGFR4-G388 cells, FGFR4-R388 cells show minimal to no inhibition of mTOR phosphorylation.

Response to everolimus

The mTOR inhibitor everolimus has shown promise for patients with progressive pNETs (20, 21). We tested BON1 cells to determine responsiveness to this drug in the context of different FGFR4 genotypes. BON1 FGFR4-G388 cells displayed the anticipated inhibition of mTOR phosphorylation in response to everolimus (Fig. 3). Consistent with reduced mTOR-mediated negative feedback inhibition, pAKT levels increased in response to everolimus. In contrast, FGFR4-R388 cells displayed relative resistance with persistently higher pmTOR levels despite drug treatment (Fig. 2). In addition, FGFR4-R388 cells revealed higher pSTAT3 levels that were also unaffected by everolimus.

To determine the biologic significance of these *in vitro* signaling differences, we tested the mTOR inhibitor in BON1 mouse xenografts. Treatment was initiated 2 weeks after inoculation when tumors measured 5 mm in diameter and continued for 30 days. At complete autopsy, no toxic changes attributable to everolimus were observed.

Although all mice developed tumors, everolimus significantly delayed growth and progression of FGFR4-G388 tumors (Fig. 3A) consistent with its recognized clinical use (20). However, no discernible effect of the drug was observed in FGFR4-R388 tumors (Fig. 3B). Median tumor burden was significantly reduced to 46% volume and 70% weight in control xenografts ($P = 0.014$) and 54% volume and 58% weight in FGFR4-G388 xenografts ($P = 0.05$). In contrast, median tumor burden was the same in untreated and drug-treated FGFR4-R388 xenografts (Fig. 3B). Western blot analysis of tumor lysates from drug-treated animals confirmed effective mTOR-phosphorylation inhibition in FGFR4-G388 but not FGFR4-R388 tumors (Fig. 3C). As documented *in vitro*, pSTAT3 levels were unaffected by everolimus treatment *in vivo*. There was no significant difference in Ki67 labeling index, apoptosis as detected by TUNEL, or N-cadherin expression between controls and treated tumors.

To validate the data suggesting a predictive value of the FGFR4 SNP in humans, we genotyped 17 patients with pNETs who had been included in a previous clinical trial of everolimus in G1 and G2 NETs and had consented to genotyping analysis (20). All patients had stage IV disease. In this group, 11 (65%) were homozygous for FGFR4-G388 and 6 (35%) carried an FGFR4-R388 allele. Of the 11 with FGFR4-G388, 7 patients had G1 tumors, 3 had G2 tumors, and 1 was of unknown grade, asthe diagnosis was based on cytology alone. Among the 6 with an FGFR4-R388 allele, 5 had a tumor graded as G1 and 1 had a G2 tumor. In an assessment of best-percentage change in RECIST tumor measurements (sum of target lesion diameters; Fig. 4A), greater reductions were observed among patients homozygous for FGFR4-G388 (mean percentage change, 25% vs. 9%; $P = 0.049$). However, due to the small sample size, the difference in partial response rate (17% vs. 27%) was not significant. Overall, median PFS among everolimus-treated patients was 14.3 (95%CI: 7.1–21.4) months. When separated by genotype, patients homozygous for FGFR4-G388 had a median PFS of 16.6 (95%CI: 10.8–22.3) months, whereas those harboring an FGFR4-R388 allele had a median of 4.8 (95%CI: NA – 10.2) months (Fig. 4B, $P = 0.40$). Median OS was 27.4 (95%CI: 7.2–47.6) months. When separated by genotype, patients homozygous for FGFR4-G388 had a median OS of 40 (95%CI: 19.5–60.5) months, whereas those harboring an FGFR4-R388 allele had a median OS of 9.3 (95%CI: NA–21.9) months (Fig. 4C, $P = 0.54$).

Discussion

Germline SNPs in coding regions have a frequency greater than 1%. Nearly half of coding SNPs cause missense mutations in corresponding proteins (22, 23). Missense SNPs may be neutral or may alter protein stability, folding, ligand binding, catalysis, regulation by allosteric mechanisms, or posttranslational modifications (24). SNPs may result in differences in

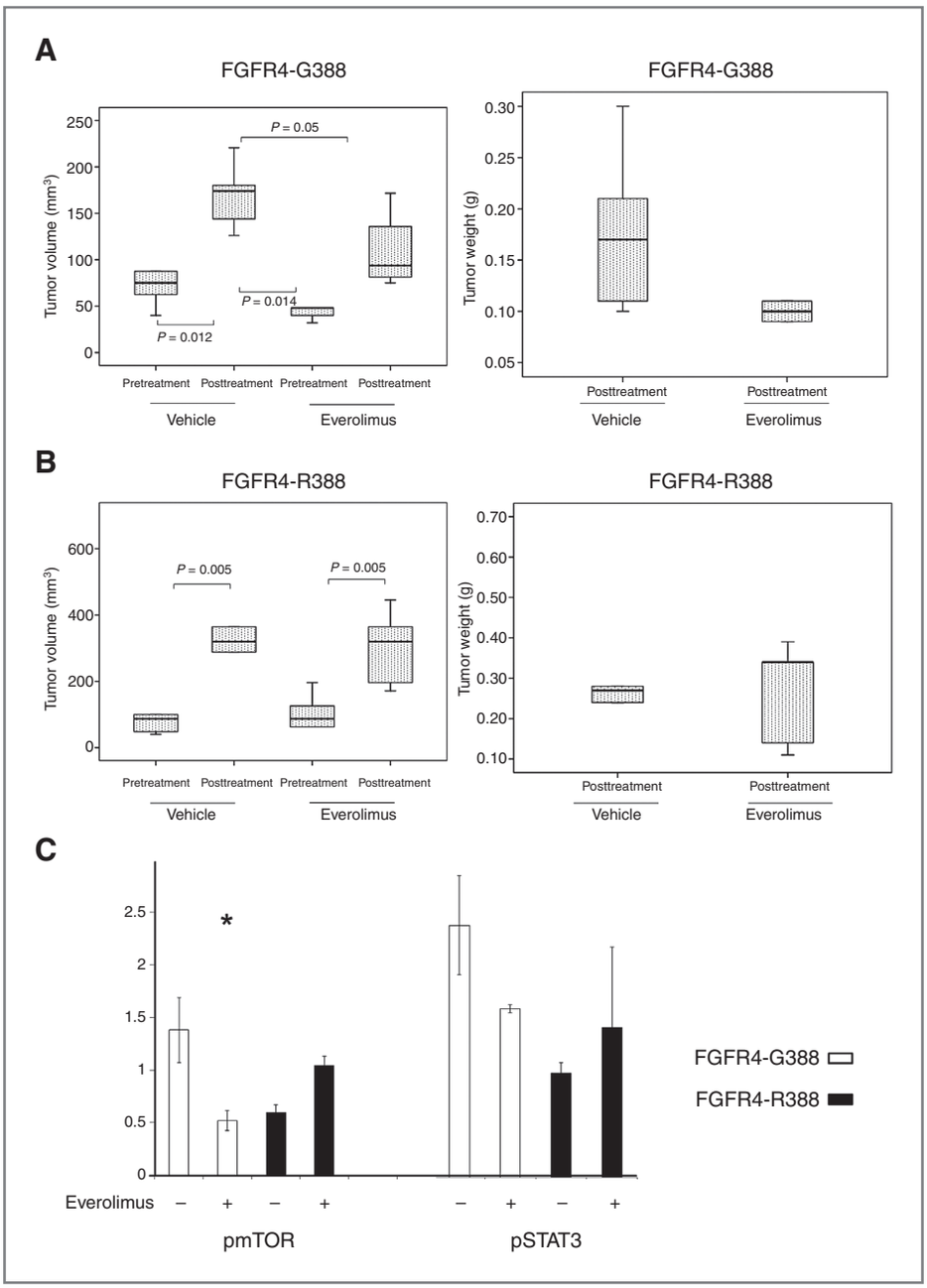

Figure 3. The effectiveness of mTOR pharmacologic inhibition is FGFR4 isoform dependent. Immunodeficient SCID mice were xenografted with BON1 tumor cells expressing FGFR4-G388 (A) or FGFR4-R388 (B) as described in Fig. 1. Pharmacologic treatments with vehicle alone or with the mTOR inhibitor everolimus (5 mg/kg) were commenced 14 days after cell inoculation as detailed under Materials and Methods. A, in animals bearing tumors expressing FGFR4-G388, tumor volumes expressed as means obtained from 5 mice in each treatment group identify statistically significant differences in response to everolimus treatment as measured by reduction in tumor volumes (left; $P < 0.05$) and tumor weights (right). B, animals bearing tumors expressing FGFR4-R388 show no appreciable change in tumor volume or tumor weight in response to everolimus treatment as indicated. C, tumor lysates from treated xenografted mice were examined by Western blotting and signals quantified by densitometric scanning. Values depicted in the bar graphs represent the mean of triplicate experiments of phosphorylated proteins adjusted for total protein of the indicated type; *, statistical significance of differences between vehicle and everolimus-treated tumors. Unlike FGFR4-G388 tumors, FGFR4-R388 tumors show no phospho-mTOR inhibition following drug therapy.

susceptibility to disease, disease outcomes, or responses to therapy.

We show that the FGFR4-G388R polymorphism significantly modifies pNET behavior: pNETs with an FGFR4-R388 allele are more commonly identified in patients with larger tumors that have local invasion, lymphovascular invasion, and lymph nodal metastases. Moreover, FGFR4-R388 is significantly associated with liver metastases, a critical prognostic feature of this disease. The small sample size of this relatively rare tumor may have reduced the power to detect more statistically significant effects of this SNP.

The biologic impact of the FGFR4 SNP was validated in experimental mouse models including an orthotopic model that recapitulates the progression of human pNETs. Human BON1 cells were selected because of their relatively unique derivation from a human pNET. Xenografts expressing FGFR4-R388 behaved in a more aggressive fashion: they were significantly larger by size and weight and exhibited greater intraperitoneal growth in the orthotopic model. Bloody ascites were noted exclusively in FGFR4-R388 tumors. Liver and lung metastases and diaphragmatic involvement were significantly more frequent in FGFR4-R388 tumors.

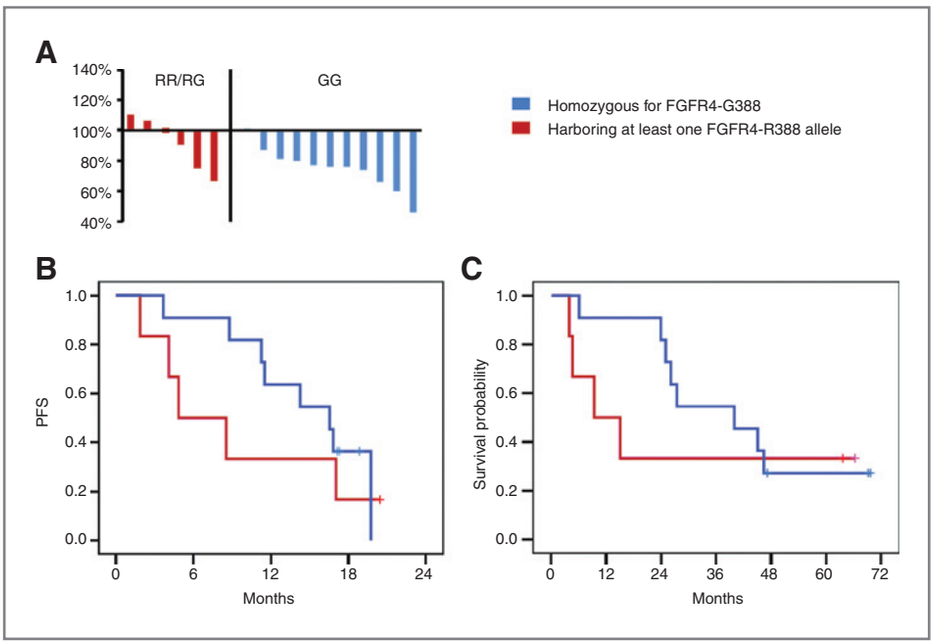

Figure 4. Clinical response to everolimus correlates with FGFR4 isoform. FGFR4 genotype was assessed in 17 patients with pNET treated with everolimus. A, waterfall plot of best response in RECIST tumor measurements. Greater reductions in tumor measurements were observed among patients homozygous for FGFR4-G388 (mean percentage decrease, 25% vs. 9%; $P = 0.049$). B, median PFS by genotype. Homozygous for FGFR4-G388, 16.6 (95% CI, 10.8–22.3) months; harboring FGFR4-R388 allele, 4.8 (95% CI, NA – 10.2) months ($P = 0.40$). C, median OS by genotype. Homozygous for FGFR4-G388, 40 (95% CI 19.5–60.5) months; harboring FGFR4-R388 allele, 9.3 (95% CI, NA – 21.9) months ($P = 0.54$).

Our data indicate that the changes in tumor behavior associated with this SNP are not mediated by changes in N-cadherin. While interactions with N-cadherin have been described with FGFR4 in pancreatic endocrine cells (17) and alterations in the extracellular domain of FGFR4 alter N-cadherin in pituitary tumors (18), the SNP that we examined here alters the transmembrane domain of FGFR4. We have recently shown that FGFR4-R388 tumors show persistently higher STAT3 phosphorylation (25), a feature that is a recognized mechanism of promoting tumor progression.

Everolimus (rapamycin, a macrolide antibiotic) exhibits potent antifungal and immunosuppressive activities by inhibiting the ability of mTOR to phosphorylate p70S6K and 4E-BP1, thereby inhibiting cell-cycle progression by reducing translation of several cell-cycle proteins including cyclin D1 and c-myc. This drug has been used successfully in the treatment of neuroendocrine carcinomas (20, 21, 26). This agent inhibited mTOR phosphorylation *in vitro* and *in vivo*, causing effective tumor suppression in FGFR4-G388 tumors. In contrast, FGFR4-R388 tumors showed persistently higher STAT3 phosphorylation despite treatment. Consistent with the well-recognized impact of STAT3 in tumor progression, persistently elevated levels of this protein in FGFR4-R388 tumors likely served to evade tumor shrinkage. These findings were tested in a retrospective analysis of patients enrolled in a previously reported clinical trial of everolimus (20). Although the numbers of patients available for analysis are small, differences in best-percentage tumor shrinkage suggest the FGFR4 genotype maybe predictive of the degree of benefit for pNET patients treated with everolimus. While the PFS and OS survival analyses were not statistically significant likely due to the small number of events, they are supportive of the prognostic role of FGFR4 genotype. Validation in a larger controlled study is needed to define the clinical use of FGFR4 genotyping.

In summary, our data show that the FGFR4-G388R polymorphism plays an important role in pNET progression and clinical aggressiveness. Further, our data indicate that the FGFR4-R388 allele encodes a receptor with distinct signaling properties that evade mTOR inhibition, providing a rational tool to predict the effectiveness of medical therapy for patients with neuroendocrine carcinomas.

Disclosure of Potential Conflicts of Interest

J.C. Yao is a consultant/advisory board member of Novartis. No potential conflicts of interest were disclosed by the other authors.

Disclaimer

The views expressed do not necessarily reflect those of the Ontario Ministry of Health and Long Term Care.

Authors' Contributions

Conception and design: S. Serra, S. Ezzat, S.L. Asa
Development of methodology: S. Serra, L. Zheng, S. Ezzat, S.L. Asa
Acquisition of data (provided animals, acquired and managed patients, provided facilities, etc.): S. Serra, L. Zheng, M.M. Hassan, A.T. Pham, J.C. Yao, S. Ezzat, S.L. Asa
Analysis and interpretation of data (e.g., statistical analysis, biostatistics, computational analysis): S. Serra, L. Zheng, M.M. Hassan, L.J. Woodhouse, J.C. Yao, S. Ezzat, S.L. Asa
Writing, review, and/or revision of the manuscript: S. Serra, M.M. Hassan, A.T. Pham, L.J. Woodhouse, J.C. Yao, S. Ezzat, S.L. Asa
Administrative, technical, or material support (i.e., reporting or organizing data, constructing databases): S. Serra, L. Zheng, J.C. Yao, S.L. Asa
Study supervision: J.C. Yao, S. Ezzat, S.L. Asa

Grant Support

This work was supported in part by the Raymond and Beverly Sackler Foundation, the Princess Margaret Hospital Foundation, and the Ontario Ministry of Health and Long Term Care.

The costs of publication of this article were defrayed in part by the payment of page charges. This article must therefore be hereby marked *advertisement* in accordance with 18 U.S.C. Section 1734 solely to indicate this fact.

Received May 31, 2012; revised August 3, 2012; accepted August 16, 2012; published OnlineFirst September 17, 2012.

References

1. Yan G, Wang F, Fukabori Y, Sussman D, Hou J, McKeehan WL. Expression and transformation of a variant of the heparin-binding fibroblast growth factor receptor (*flg*) gene resulting from splicing of the exon at alternate 3′-acceptor site. Biochem Biophys Res Commun 1992;183:423–430.
2. Ornitz DM, Zu J, Colvin JS, McEwen DG, MacArthur CA, Coulier F, et al. Receptor specificity of the fibroblast growth factor family. J Biol Chem 1996;271:15292–7.
3. Givol D, Yayon A. Complexity of FGF receptors: genetic basis for structural diversity and functional specificity. FASEB J 1992;6:3362–9.
4. Passos-Bueno MR, Wilcox WR, Jabs EW, Sertie AL, Alonso LG, Kitoh H. Clinical spectrum of fibroblast growth factor receptor mutations. Hum Mutat 1999;14:115–25.
5. Xiao S, Nalabolu SR, Aster JC, Ma J, Abruzzo L, Jaffe ES, et al. FGFR1 is fused with a novel zinc-finger gene, ZNF198, in the t(8;13) leukaemia/lymphoma syndrome. Nat Genet 1998;18:84–7.
6. Taylor JG, Cheuk AT, Tsang PS, Chung JY, Song YK, Desai K, et al. Identification of FGFR4-activating mutations in human rhabdomyosarcomas that promote metastasis in xenotransplanted models. J Clin Invest 2009;119:3395–407.
7. Eswarakumar VP, Lax I, Schlessinger J. Cellular signaling by fibroblast growth factor receptors. Cytokine Growth Factor Rev 2005;16:139–49.
8. Jaakkola S, Salmikangas P, Nylund S, Partanen J, Armstrong E, Pyrhonen S, et al. Amplification of FGFR4 gene in human breast and gynecological cancers. Int J Cancer 1993;54:378–82.
9. Bange J, Prechtl D, Cheburkin Y, Specht K, Harbeck N, Schmitt M, et al. Cancer progression and tumor cell motility are associated with the FGFR4 Arg(388) allele. Cancer Res 2002;62:840–7.
10. Morimoto Y, Ozaki T, Ouchida M, Umehara N, Ohata N, Yoshida A, et al. Single nucleotide polymorphism in fibroblast growth factor receptor 4 at codon 388 is associated with prognosis in high-grade soft tissue sarcoma. Cancer 2003;98:2245–50.
11. Wang J, Stockton DW, Ittmann M. The fibroblast growth factor receptor-4 Arg388 allele is associated with prostate cancer initiation and progression. Clin Cancer Res 2004;10:6169–78.
12. Falvella FS, Frullanti E, Galvan A, Spinola M, Noci S, De Cecco L, et al. FGFR4 Gly388Arg polymorphism may affect the clinical stage of patients with lung cancer by modulating the transcriptional profile of normal lung. Int J Cancer 2009;124:2880–5.
13. Sasaki H, Okuda K, Kawano O, Yukiue H, Yano M, Fujii Y. Fibroblast growth factor receptor 4 mutation and polymorphism in Japanese lung cancer. Oncol Rep 2008;20:1125–30.
14. da Costa Andrade V, Parise O Jr, Hors CP, de Melo Martins PC, Silva AP, Garicochea B. The fibroblast growth factor receptor 4 (FGFR4) Arg388 allele correlates with survival in head and neck squamous cell carcinoma. Exp Mol Pathol 2007;82:53–57.
15. Thussbas C, Nahrig J, Streit S, Bange J, Kriner M, Kates R, et al. FGFR4 Arg388 allele is associated with resistance to adjuvant therapy in primary breast cancer. J Clin Oncol 2006;24:3747–55.
16. Seitzer N, Mayr T, Streit S, Ullrich A. A single nucleotide change in the mouse genome accelerates breast cancer progression. Cancer Res 2010;70:802–12.
17. Cavallaro U, Niedermeyer J, Fuxa M, Christofori G. N-CAM modulates tumour-cell adhesion to matrix by inducing FGF-receptor signalling. Nat Cell Biol 2001;3:650–7.
18. Ezzat S, Zheng L, Asa SL. Pituitary tumor-derived fibroblast growth factor receptor 4 isoform disrupts neural cell-adhesion molecule/N-cadherin signaling to diminish cell adhesiveness: a mechanism underlying pituitary neoplasia. Mol Endocrinol 2004;18:2543–52.
19. Klimstra DS, Arnold R, Capella C, Hruban RH, Kloppel G, Komminoth P, et al. Neuroendocrine neoplasms of the pancreas. In:Bosman FT, Carneiro F, Hruban RH, Theise ND, editors. WHO classification of tumours of the digestive system. Lyon: IARC Press; 2010.p. 322–326.
20. Yao JC, Phan AT, Chang DZ, Wolff RA, Hess K, Gupta S, et al. Efficacy of RAD001 (everolimus) and octreotide LAR in advanced low- to intermediate-grade neuroendocrine tumors: results of a phase II study. J Clin Oncol 2008;26:4311–8.
21. Yao JC, Shah MH, Ito T, Bohas CL, Wolin EM, Van Cutsem E, et al. Everolimus for advanced pancreatic neuroendocrine tumors. N Engl J Med 2011;64:514–23.
22. Ng PC, Henikoff S. Predicting the effects of amino acid substitutions on protein function. Annu Rev Genomics Hum Genet 2006;7:1–80.
23. Bromberg Y, Rost B. Correlating protein function and stability through the analysis of single amino acid substitutions. BMC Bioinformatics 2009;10(Suppl 8):S8.
24. Wang Z, Moult J. SNPs, protein structure, and disease. Hum Mutat 2001;17:263–70.
25. Tateno T, Asa SL, Zheng L, Mayr T, Ullrich A, Ezzat S. The FGFR4-G388R polymorphism promotes mitochondrial STAT3 serine phosphorylation to facilitate pituitary growth hormone cell tumorigenesis. PLoS Genet 2011;7:e1002400.
26. Pavel ME, Hainsworth J D, Baudin E, Peeters M, Horsch D, Winkler RE, et al. Everolimus plus octreotide long-acting repeatable for the treatment of advanced neuroendocrine tumours associated with carcinoid syndrome (RADIANT-2): a randomised, placebo-controlled, phase 3 study. Lancet 2011;378:2005–12.